MITO: A new operational model for the forecasting of the Mediterranean sea circulation

E. Napolitano*†, R. Iacono†, M. Palma†, G. Sannino†, A. Carillo†,
E. Lombardi†, G. Pisacane† and M. V. Struglia†

Climate Modeling Laboratory, Division Model and Technologies for Risk Reduction, Department for
Sustainability, ENEA, Rome, Italy

Availability of detailed short-term forecasts of the ocean main characteristics (circulation and waves) is essential for a correct management of the human activities insisting on coastal areas. These activities include the extraction of renewable energy, which has developed in recent years, and will play an important role in the context of future blue growth. The present work describes the implementation of a new ocean operational system, named MITO, that provides daily 5 days forecasts of the Mediterranean Sea circulation. Distinctive features of this system are the inclusion of the main effects of the tidal forcing, both local and propagating from the Atlantic, and the high spatial detail. The horizontal resolution is of 1/48° (about 2 km) in most of the computational domain, and is smoothly increased (down to few hundred meters) in key passages, such as the Gibraltar Strait and the Turkish Straits, to correctly resolve the complex local dynamics. Initial and boundary conditions for MITO are taken from the reference European operation model of Copernicus, which covers the Mediterranean Sea with a uniform resolution of 1/24°. A thorough validation of the new system is performed, analyzing the forecasts of the year 2020, whose results are compared with *in situ* and remote observational data (sea surface temperature, altimeter data, temperature and salinity profiles by floats, tide-gauge measurements, available through the Copernicus portal) using the same large-scale metrics applied in the validation of the Copernicus operational model. MITO results are generally found in very good agreement with the observations, despite the fact that the model does not make explicit use of data assimilation. We also give examples of the capability of the model to correctly describe complex local mesoscale dynamics, and point out aspects that need to be improved, which will be addressed in a future upgrade of the operational implementation.

Introduction

Correct planning and management of the economic activities insisting on marine coastal areas is essential to reduce the impacts on the local ecosystems, and, in some cases, to preserve the resources being exploited. This is a key issue for a country like Italy, with more than 8,000 km of coastline, where a significant portion of the gross domestic product derives from activities taking place in coastal areas. Together with marine transportation, tourism, fishing, and aquaculture, these activities now include the extraction of renewable energy, which has developed in recent years, under the impulse of the "blue growth" policies adopted at the European level (https://blue-action.eu/policy-feed/blue-growth).

A recent assessment of the energy potential in the Mediterranean Sea, with focus on coastal areas, has been given by Nikolaidis et al. (2019), who presented results of the Interreg MED project Maestrale (https://maestrale.interreg-med.eu). It was found that the most promising fonts are the offshore wind energy and the wave energy, which can be extracted both offshore, using floating devices (see, e.g., Pisacane et al., 2018, and references therein), and on shore, with devices embedded in ports or wave-breakers (e. g., Barbarelli et al., 2018). Other potentially interesting fonts are the thermal energy (here temperature differences between air and sea, or between different ocean layers are exploited), and the energy residing in marine currents with a strong tidal component. Interesting locations for the latter font are in the Messina (Coiro et al., 2013) and Gibraltar Straits, and in a few coastal sites in the Aegean Sea. Another font of potential interest relies on the exploitation of salinity gradients due to river discharges, but the technologies in this field have not yet reached a mature stage.

It can be easily understood that activities aimed at harvesting energy from these fonts do require a detailed knowledge of the marine environment, both in terms of circulation and sea state (waves), on a variety of time scales. Multidecadal simulations of the past climate, and of future climate, under different emission scenarios, are necessary to assess the resources and their variability, and consequently to choose the best technological solutions. On the other hand, the optimization and management of the devices being deployed requires the availability of detailed and reliable short-term forecasts.

In the last 2 decades, forecasting of the marine circulation has received increasing attention, thanks to the development of the operational oceanography (e.g., Schiller and Brassington, 2011; Davidson et al., 2019), a branch of oceanography whose purpose is to develop observational networks and numerical forecasting systems to be used for an accurate prediction of the short-term evolution of the main ocean physical parameters (currents, temperature, salinity), similarly to what has been done for long time for the atmosphere (weather forecasting). A recent ample review of developments in this relatively new field,

focusing on European seas, is given in Fernandez et al. (2021), which contains the Proceedings of the 9th EuroGOOS Conference (EuroGOOS is the European branch of GOOS, the intergovernmental Global Ocean Observing System), devoted to "Advances in operational oceanography: expanding Europe's ocean observing and forecasting capacity".

Current operational ocean forecasts are mainly "deterministic"; they are based on a single high-resolution simulation that starts from the "best" possible initial condition, that is, an initial three-dimensional sea state that is as close as possible to the available observations, in terms of some given metrics. *A posteriori*, simulations of reanalysis are also made, by constraining the numerical models with new observational data that have become available, through sophisticated numerical techniques of data assimilation analogous to those initially developed in the atmospheric context.

Models for the ocean forecast and reanalysis are being constantly improved, building on the advances in the numerical modelling techniques, on the developments in the field of high-performance computing, and on the growing amount of observations, both *in-situ* and from satellite. At European level, most of these observations are collected by the Copernicus Marine Environment Monitoring Service (CMEMS; https://marine.copernicus.eu/it), the marine component of the Copernicus Programme of the European Union, which makes these data freely available to the interested research community. The CMEMS repository also contains state of the art modelling products for the European seas, which can be used as reference in the development of new products, and for the nesting with regional models of higher spatial resolution.

In the Italian context, several operational models for the forecast of the circulation have been developed in the last 2 decades, both for the whole Mediterranean basin (Oddo et al., 2009), and for some Italian seas (Tyrrhenian Sea, Adriatic Sea, Western Mediterranean, Sicily Strait), which have been part of a national network coordinated by the National Group for Operational Oceanography (GNOO; see Napolitano et al., 2016). Some of these developments (see Napolitano et al., 2014), together with those that are the subject of the present paper, have been carried out at ENEA (the National Agency for New Technologies, Energy and Sustainable Economic Development), in the context of a long-term agreement with the Italian Ministry of Economic Development (MISE) that has promoted research activities in the energy sector.

In this work, we describe a new, high-resolution (horizontal grid spacing of 1/48°, or about 2 km) operational system for the forecasting of the Mediterranean Sea circulation we have recently developed, and perform a detailed assessment of its skills. The system is named MITO (MIT Operational), since its computational core is based on an implementation of the MITgcm ocean model (Marshall et al., 1997a; Marshall et al., 1997b) of the

Massachusetts Institute of Technology. An important new feature that we have added to the basic computational core in this implementation is the main tidal forcing, both local, as a body force, and propagating from the Atlantic through the Gibraltar Strait. This was one of the main motivations for the development of MITO, since, when this development started, there was no model for the forecast of the Mediterranean circulation including tidal effects. Moreover, in the first studies with the new model (Palma et al., 2020), we found that complex, nonlinear effects of the tides on the dynamics were present in several regions of the Mediterranean Sea. This means that tidal effects cannot be linearly superposed *a posteriori*; they need to be included in forecasting models at basin scale to have a correct description of the dynamics, and, eventually, to provide the correct boundary conditions to higher resolution regional models.

We shall assess the performance of MITO by comparing the results of the forecasts of the year 2020 with *in situ* and remote experimental observations (sea surface temperature, altimeter data, temperature and salinity profiles by floats, tide-gauge measurements) available through CMEMS. The comparison will make use of the same large-scale metrics applied in the validation of the reference Mediterranean operational model of CMEMS (NEMO; Clementi et al., 2021). The current version of the model produce forecasts at 1/24° of horizontal resolution with 141 vertical levels and includes current-wave interactions, and, from 2021 on, tidal forcing.

The paper is organized as follows. The main features of the model and of its operational implementation are described in *MITO system: Main model features and operational details* Section, whereas Sections 3-6 are concerned with the system validation and the analysis of some interesting aspects of the 2020 Mediterranean circulation. In particular, *Sea surface temperature* Section focuses on the sea surface temperature, and *Hydrological profiles* Section on the hydrological properties. *Circulation* Section examines the large-scale surface circulation patterns produced by the system, and gives some examples of the model capability of capturing small-scale mesoscale features. *Sea level* Section focuses on sea level, both in open sea and in coastal areas, and *Conclusion* Section presents the conclusions, indicating aspects that should be examined to further improve the skill of the system.

MITO system: Main model features and operational details

The MITO forecasting system is based on an innovative, tide-including, three-dimensional numerical model of the marine circulation, implemented on a domain that covers the whole Mediterranean Sea-Black Sea system. The model has 100 vertical z-levels, and a horizontal resolution of 1/48° (about 2 km) over most of the computational domain. MITO is therefore an eddy-

resolving model, since the typical Rossby radius of deformation for the Mediterranean is of 10–15 km. Note that the horizontal resolution is higher than that of the current NEMO-CMEMS-Copernicus forecasting model of the Mediterranean Sea (Clementi et al., 2021). A key feature of MITO is the fact that the horizontal resolution is smoothly increased in some critical regions, namely the Strait of Gibraltar and the Turkish Straits. At the Gibraltar Strait, a very high horizontal detail is achieved (down to 200 m) that allows to adequately resolve the complex local dynamics, including the propagation of the Atlantic tidal signal into the Mediterranean basin. Further information on the model and its implementation can be found in Palma et al. (2020), where a first assessment of the main effects of tidal forcing on the circulation was performed. Tidal forcing includes both the tide generating potential as a body force in the momentum equations and the tidal signal propagating from the Atlantic Ocean (see Naranjo et al., 2014, and Sannino et al., 2015, for further details). The four main lunar, solar, and luni-solar tidal components (M2, O1, S2, K1) have been prescribed inside the computational domain.

The model is initialized and forced at the Atlantic boundary by temperature and salinity data from the NEMO-CMEMS model (details are given in *MITO system: Main model features and operational details* Section of Palma et al., 2020).

Data from the high-resolution (5 km), non-hydrostatic SKIRON/Eta regional atmospheric model (Kallos et al., 1997) are used to compute the atmospheric forcing at the sea surface (hourly wind stress, heat and fresh water fluxes). SKIRON is part of the POSEIDON forecast system, which is operational at the National and Kapodistrian University of Athens (http://forecast.uoa.gr/forecastnewinfo.php). The performances of the last version of the model, with respect to those of a previous implementation with horizontal resolution of 10 km have been assessed in Papadopoulos and Katsafados (2009). It is a well-established model that has been used in variety of investigations of atmosphere and ocean dynamics (see, e.g., Kallos et al., 2006; Stathopoulos et al., 2013; de Ruggiero et al., 2016) in the last 2 decades.

The current version of the system does not explicitly implement a data assimilation scheme, although the initial and boundary conditions from the NEMO-CMEMS model incorporate observed data of sea level, temperature and salinity, thus mildly constraining the forecast [the NEMO-CMEMS model solutions are corrected by a variational data assimilation scheme (3DVAR) of temperature and salinity vertical profiles and along track satellite Sea Level Anomaly observations; Clementi et al., 2021, also objective analysis of the SST is used to correct the surface heat fluxes]. We found that this is sufficient to keep the forecasts close to the observations, although future developments envisage the implementation of assimilation procedures, to further improve the skill.
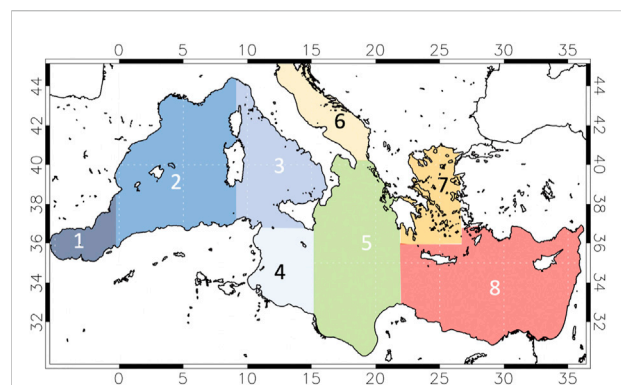
The MITO operational system consists of a complex set of numerical codes, implemented on ENEA's High-Performance
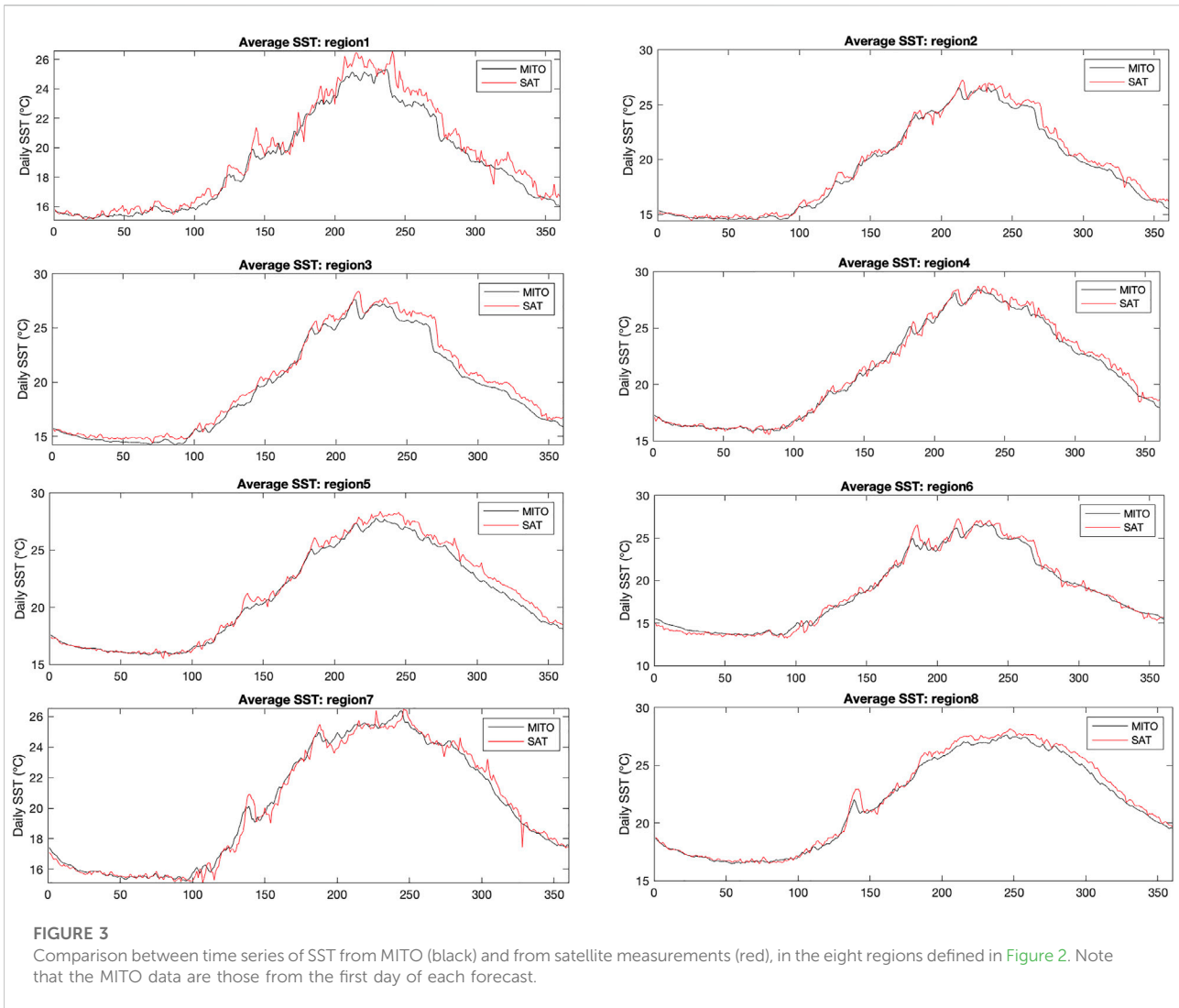
FIGURE 1
MITO operational chain.
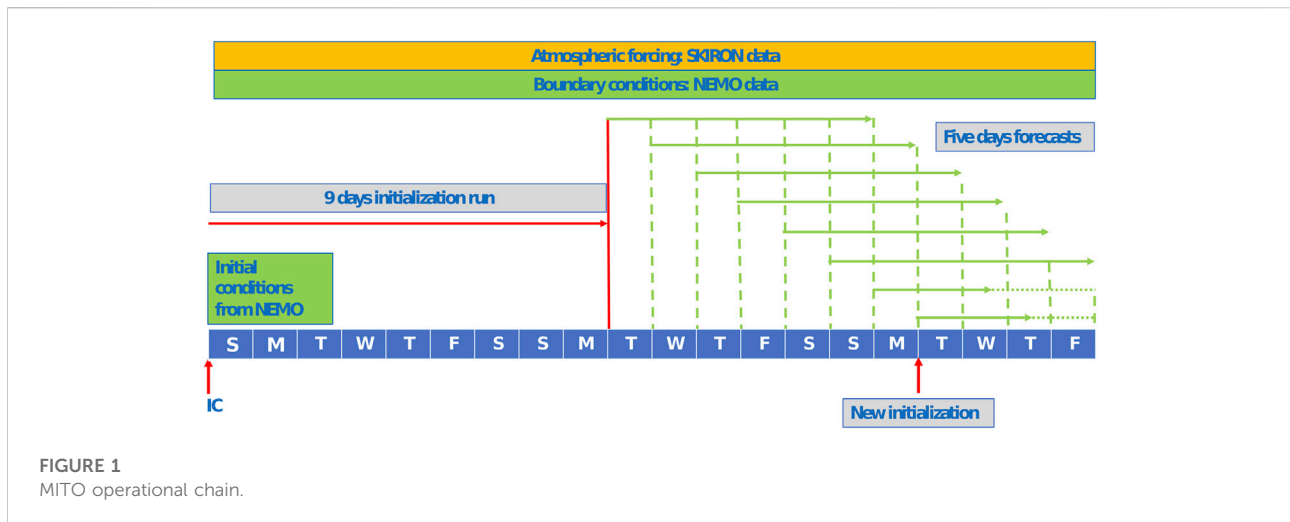
Computing (HPC) infrastructures. The operational chain is schematized in Figure 1. Every Tuesday the model is initialized with data from the NEMO-CMEMS Mediterranean Sea and Black Sea forecast models, and a 14-days run is performed, of which the first 9 days represent the initialization phase (forced by SKIRON, here we use the first days of the Skiron forecasts that are assumed to have the best skills) and the last five are the actual forecast. In each of the following days (from Wednesday to next Monday) a 5 days forecast is performed, initialized with restart files from the previous run (see the scheme in Figure 1). The choice of 9 days for the initial adjustment results from an evaluation of the time needed for damping spurious barotropic waves in the different sub-basins. Such perturbations are unavoidable, because they result from the inconsistency between the initial conditions and MITO bathymetry. Nine days are sufficient to completely damp the initial perturbations, and allow for a correct development of the baroclinic velocity field (e.g., Ezer and Mellor, 1994; remember that we initialize with the hydrological fields). The whole operational chain is repeated every week.

Data

The operational forecasting system produces every day hourly datasets of currents (3D), free surface height (SSH; 1D), and hydrological variables (temperature—T - and salinity—S; 3D), for the following 5 days. The datasets are in NetCDF-4 format, a format widely used in the ocean modelling community. The validation makes use of the first day of each forecast, which is expected to have the best skill. The following data from CMEMS are used to assess the skill of the system:

FIGURE 2
Regions on which statistical analyses for the SST, SSH and the hydrological variables have been carried out.

- Sea Surface Temperature (SST) measured from satellite; product SST_MED_SST_L4_NRT_OBSERVATIONS_010_004, which is provided on a regular grid at 1/16°, and represents the reconstruction of the daily SST based on the data measured at 0:00 UTC using various types of sensors (Buongiorno Nardelli et al., 2013);
- Vertical profiles of temperature and salinity obtained from Argo floaters (product INSITU_MED_NRT_OBSERVATIONS_013_035; data provided by the European Research Infrastructure Consortium);
- Absolute Dynamic Topography (ADT) measured from satellite altimeters, and corresponding geostrophic reconstructions of the circulation [product SEALEVEL_EUR_PHY_L4_MY_008_068; data

FIGURE 3
Comparison between time series of SST from MITO (black) and from satellite measurements (red), in the eight regions defined in Figure 2. Note that the MITO data are those from the first day of each forecast.

processed by SSALTO/DUACS and distributed by AVISO+ (https://www.aviso.altimetry.fr) with support from CNES (Centre national d'études spatiales; France)];

- Sea level data from coastal tide-gauge stations (product INSITU_MED_NRT_OBSERVATIONS_013_035);
- Turbidity data from satellite (product OCEANCOLOUR_MED_OPTICS_L3_REP_OBSERVATIONS_009_095).

The comparison between the model forecasts and the observations has been done for the whole 2020, for the eight regions shown in Figure 2, which are considered as dynamically coherent. The operational system has been validated via the same method adopted for the CMEMS forecasting system (Clementi et al., 2021), which makes use of the bias between the predicted and observed values,

TABLE 1 Bias and RMSD of the SST [°C]–(MITO vs. satellite data).

Region	Mean	RMSD
1	−0.46	0.71
2	−0.31	0.51
3	−0.51	0.68
4	−0.19	0.42
5	−0.37	0.55
6	−0.06	0.55
7	0.01	0.42
8	−0.30	0.45

and of the corresponding root-mean-square deviation (RMSD), as the main statistical metrics to assess the reliability of the relevant predicted variables.

FIGURE 4
The SST diurnal Cycle for Mediterranean Basin Gulf of Lion and the Southern Tyrrhenian sea.

FIGURE 5
Spatial distribution of the Argo profiles available in 2020 (period March-December).
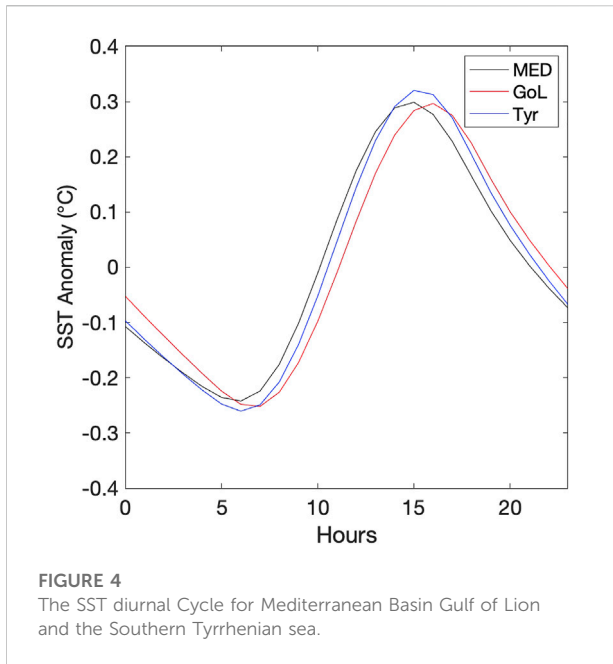
Sea surface temperature

The comparison between modeled and observed daily series of SST (values taken at 00 UTC for both) for the eight regions is shown in Figure 3. There is generally a good agreement between model data and observations, even though in some regions the model SST underestimates the observed one in the second half of the year.

The corresponding bias and RMSD values are reported in Table 1. The bias is always below 0.5°C, except for region 3 (Tyrrhenian-Ligurian), where it is slightly larger, and it is almost always negative. The best agreement is found in the Aegean Sea (7) and the Levantine basin (8). Discrepancies can be attributable to deficiencies either in the data (L4 data making use of climatologic values to fill missing data) or in the forecasts, as a consequence of the approximations implied by the use of vertical mixing parameterizations and bulk formulas.

The diurnal variation of the SST is a topic that has recently received considerable attention, since it has been shown that resolving this variation may have a non-negligible impact on the estimation of the total mean heat budget in the Mediterranean Sea (Marullo et al., 2016). The SST diurnal cycle also controls biogeochemical processes in the upper ocean and in coastal ecosystems (e.g., Doney et al., 1995; Zhang et al., 2022). Figure 4 shows the SST diurnal cycle as reproduced by the model for August 2020, averaged over the whole Mediterranean basin (black curve), which is in good qualitative agreement with that obtained by Marullo et al. (2016) for the summer of 2011. The red curve corresponds to the analogous cycle for the Gulf of Lion and the blue one to that
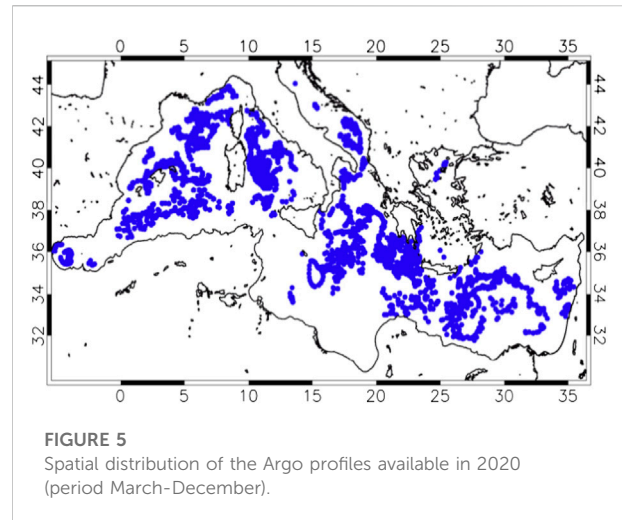
TABLE 2 Bias (MITO-observation) and RMSD for temperature (in °C) and salinity (psu).

Layer (m)	T		S	
	Bias	RMSD	Bias	RMSD
0–10	−0.224	1.049	−0.154	0.316
10–30	−0.079	1.573	−0.138	0.301
30–60	0.363	1.795	−0.140	0.297
60–100	0.275	1.067	−0.137	0.298
100–150	0.132	0.586	0.051	0.217
150–300	−0.006	0.390	0.020	0.173
300–600	−0.112	0.240	0.017	0.095
600–1,000	−0.098	0.175	0.020	0.096
1,000–2000	−0.188	0.202	0.014	0.090

of the southeastern Tyrrhenian Sea, with the latter displaying the largest amplitude. This is an area where diurnal warming events have been observed in the past (Marullo et al., 2016).

Hydrological profiles

The vertical profiles of temperature and salinity produced by the model have been compared with Argo profiles The number of available profiles for 2020 is 2,993. These profiles are quite regularly distributed over the period from March to December; their spatial distribution is displayed in Figure 5. For each observed profile, the corresponding modelled one was extracted at the nearest grid point and output time.

The average bias and RSMD for temperature and salinity are reported in Table 2, for nine reference layers in the first 2000 m of

TABLE 3 Bias (MITO-observation) for temperature (A) and salinity (B): monthly variability. The nine reference layers considered are indicated in the first column.

A	Mar	Apr	May	Jun	Jul	Aug	Sept	Oct	Nov	Dec
0–10	−0.044	−0.246	−0.369	−0.347	−0.165	−0.205	−0.451	0.084	−0.299	−0.093
10–30	−0.007	−0.134	−0.118	−0.166	0.080	0.245	−0.339	0.102	−0.272	−0.085
30–60	0.117	0.063	0.311	0.711	0.670	1.009	0.404	0.523	−0.170	0.007
60–100	0.166	0.117	0.288	0.411	0.401	0.573	0.367	0.364	−0.051	0.140
100–150	0.136	0.094	0.217	0.214	0.199	0.246	0.222	0.116	−0.089	0.038
150–300	0.032	0.008	0.027	0.021	−0.017	−0.007	0.057	−0.001	−0.098	−0.044
300–600	−0.089	−0.098	−0.085	−0.104	−0.099	−0.115	−0.099	−0.128	−0.139	−0.138
600–1,000	−0.079	−0.082	−0.086	−0.100	−0.079	−0.098	−0.088	−0.124	−0.101	−0.123
1,000–2000	−0.191	−0.185	−0.182	−0.193	−0.181	−0.193	−0.187	−0.188	−0.188	−0.195

B	Mar	Apr	May	Jun	Jul	Aug	Sept	Oct	Nov	Dec
0–10	−0.155	−0.162	−0.122	−0.172	−0.166	−0.176	−0.128	−0.126	−0.087	−0.168
10–30	−0.141	−0.153	−0.135	−0.164	−0.159	−0.157	−0.137	−0.127	−0.091	−0.145
30–60	−0.146	−0.158	−0.170	−0.159	−0.150	−0.153	−0.092	−0.096	−0.083	−0.127
60–100	−0.139	−0.145	−0.147	−0.134	−0.118	−0.159	−0.084	−0.103	−0.016	−0.083
100–150	−0.047	−0.058	−0.092	−0.048	−0.020	−0.052	−0.030	−0.007	0.059	0.001
150–300	0.028	0.015	0.001	0.033	0.019	0.031	0.047	0.054	0.060	0.019
300–600	−0.013	0.013	0.027	0.033	0.021	0.014	0.022	0.012	0.014	0.011
600–1,000	0.016	0.014	0.022	0.025	0.020	0.013	0.018	0.004	0.013	0.007
1,000–2000	0.004	0.014	0.027	0.037	0.032	0.025	0.026	0.020	0.028	0.026

FIGURE 6
Average 2020 circulation in the western and central Mediterranean. MITO circulation at 30 m of depth in the left panels; geostrophic reconstruction from altimeter data (AVISO) in the right panels.
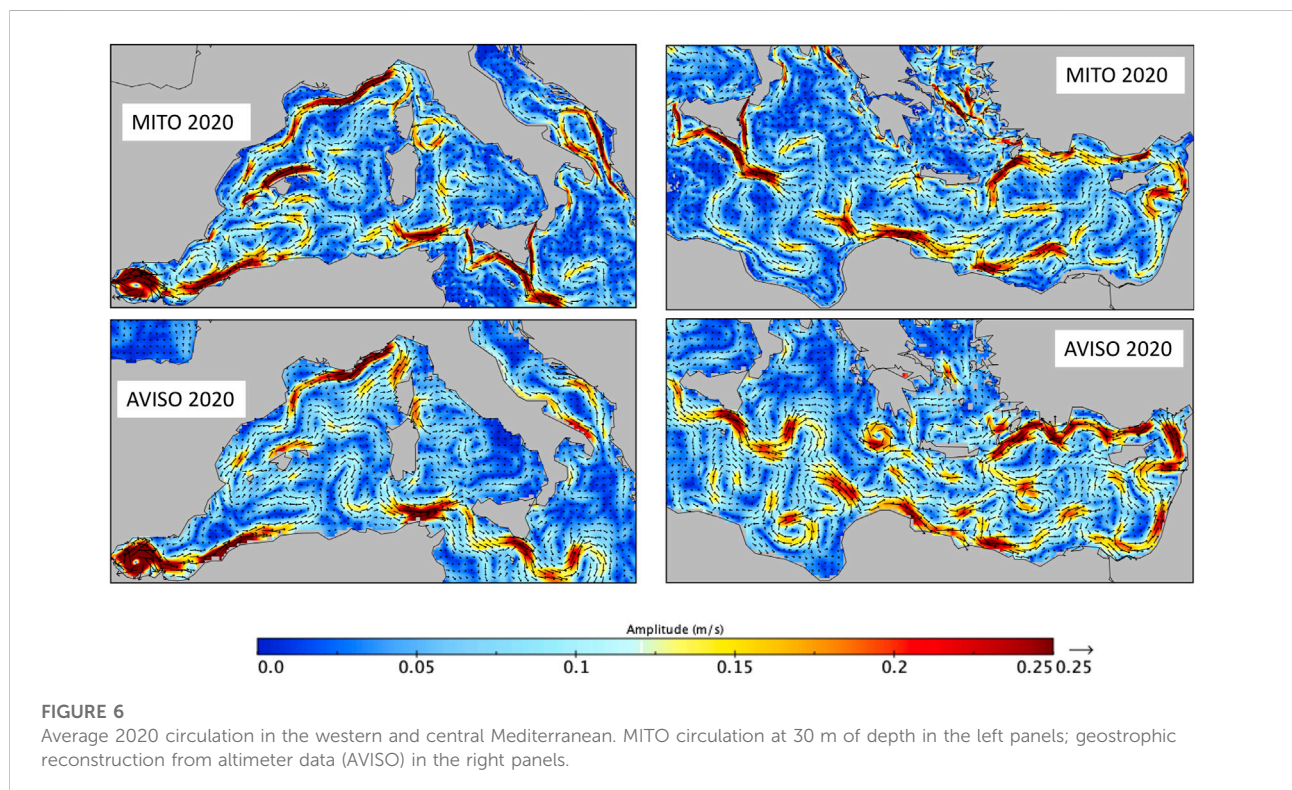
the water column. In the first 30 m model temperatures are lower than those observed, consistently with the results obtained for SST (Section 2.2). Between 60 and 150 m, the bias is slightly higher and changes sign, to reverse again in the deep layers. Model salinity is generally lower than the observations in the surface layers.

The monthly biases computed for temperature (A) and salinity (B) are shown in Table 3. The temperature bias exhibits moderate seasonal variability; it is higher in spring and summer and quite low in December and March. The corresponding values for salinity do not indicate significant variations along the year.

Circulation

Surface circulation

The annual averages of the surface circulation (30 m of depth) for the western and eastern basins are shown in Figure 6 (upper panels), and compared with the average geostrophic flow reconstruction by AVISO (lower panels). It can be seen that the model reproduces all the well-known circulation features of the western basin, namely: the Algerian Current, the Liguro-Provençal Current, the cyclonic gyre in the Gulf of Lion, the cyclone-anticyclone dipole in the north Tyrrhenian, the Atlantic Ionian Stream (AIS), which meanders in the channel of Sicily, the anticyclonic region in the south of the Ionian, and the cyclonic gyre of the south Adriatic. The model features are in very good agreement with those present in the average geostrophic flow. There are some differences, however. Currents tend to be stronger in the model circulation, which is something that could be expected, because the model resolution is much higher than that of the altimeter maps, and we can consequently resolve mesoscale dynamics that are not well captured in the latter. Moreover, the model includes ageostrophic dynamics induced by nonlinear advection and wind-driven dynamics that are missing in the altimetric reconstruction. There are also local details not resolved in the average geostrophic reconstruction. An example is the current, with a strong tidal component, that originates in the Messina Strait (the very narrow passage between the eastern tip of Sicily and the western tip of Calabria, in the southern Italy) and borders the eastern coast of Sicily.

Results for the eastern Mediterranean are also very good. Here we recognize the Ionian current that enters the Levantine and flows cyclonically along the coasts of the basin, forming large meanders including mesoscale structures. The model also reproduces well the cyclonic region represented by the gyre of Rhodes and the anticyclonic gyres such as Mersha Mathrut, Shikmona, and Ierapetra.
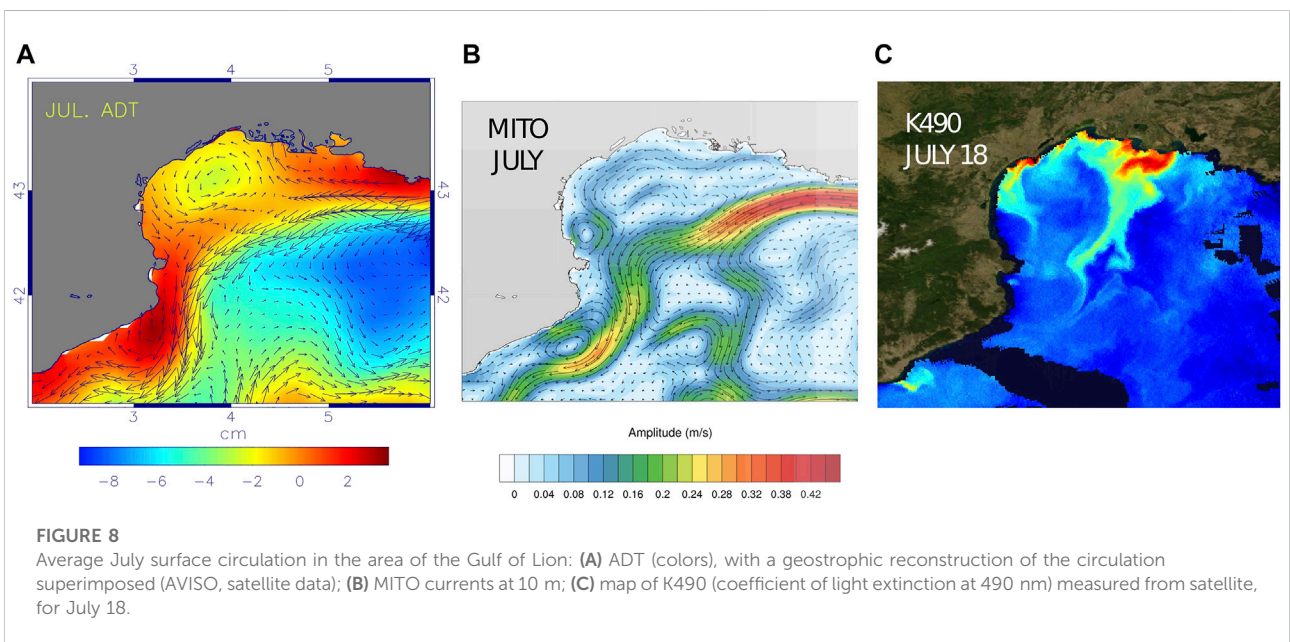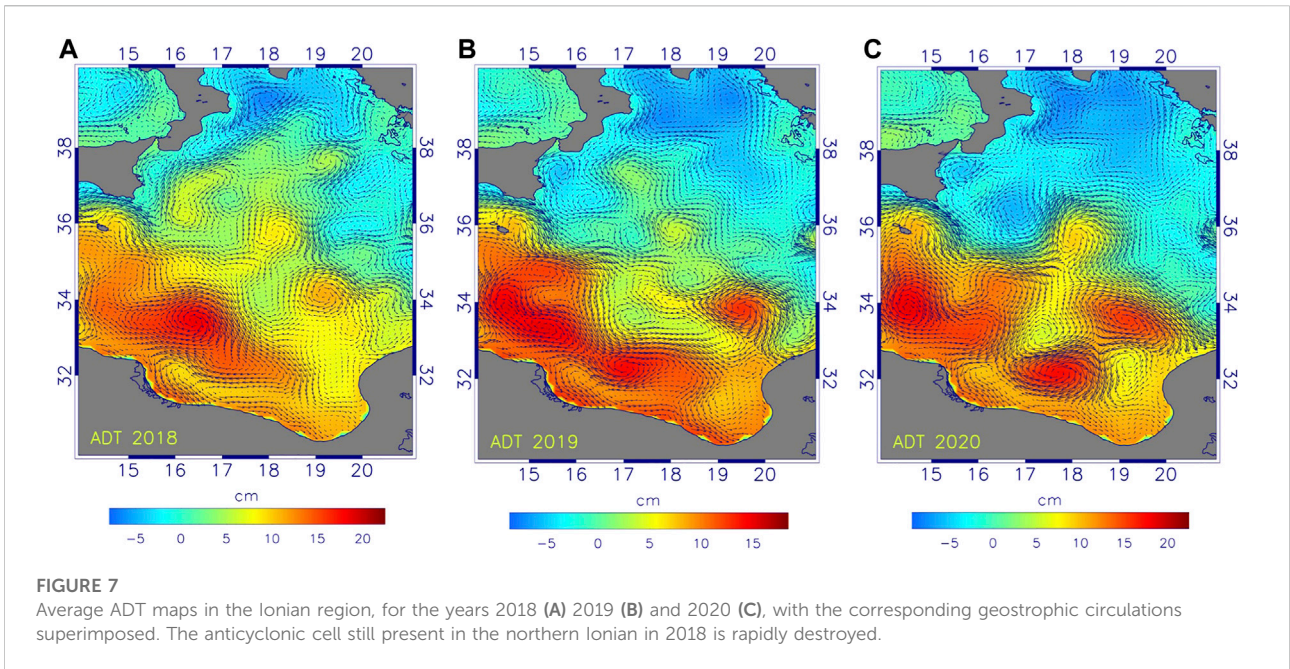
It is interesting to note that both the model circulation and the geostrophic reconstruction from satellite data indicate the presence of an overall cyclonic circulation in the northern Ionian. This region has recently been the focus of many investigations (e.g., Borzelli et al., 2009; Menna et al., 2019; Notarstefano et al., 2019), because of the presence of the so-called North Ionian Gyre (NIG) oscillation, a periodic reversal of the circulation, observed a few times in the last decades, which appears to have a nearly decadal time scale. This phenomenon, whose causes are not yet entirely clear, influences the transport of less salty surface water in the Levantine basin. ADT maps for the Ionian Sea, for the years from 2018 to 2020, with the corresponding geostrophic reconstructions of the circulation superimposed, are displayed in Figure 7. The figure shows that the anticyclonic cell intruding the north Ionian (above 36°N, and approximately in the range 16°–19°E), still present in 2018, becomes weak in 2019, where a cyclonic cell starts to grow. The latter becomes dominant in 2020, filling the whole north Ionian, and the Atlantic Ionian Stream (AIS) coming from the Sicily Channel directly flows in the middle Ionian, heading towards the Levantine basin. This indicates that the third anticyclonic phase of the NIG (Menna et al., 2019; Notarstefano et al., 2019) has apparently lasted only a few years.

Examples of local dynamics

An example of the effects of high resolution is given in Figure 8, where we compare the average circulation of July 2020 in the Gulf of Lion, at 10 m, produced by MITO (b) with the July average of the ADT in the area, with the corresponding geostrophic circulation superimposed (a).
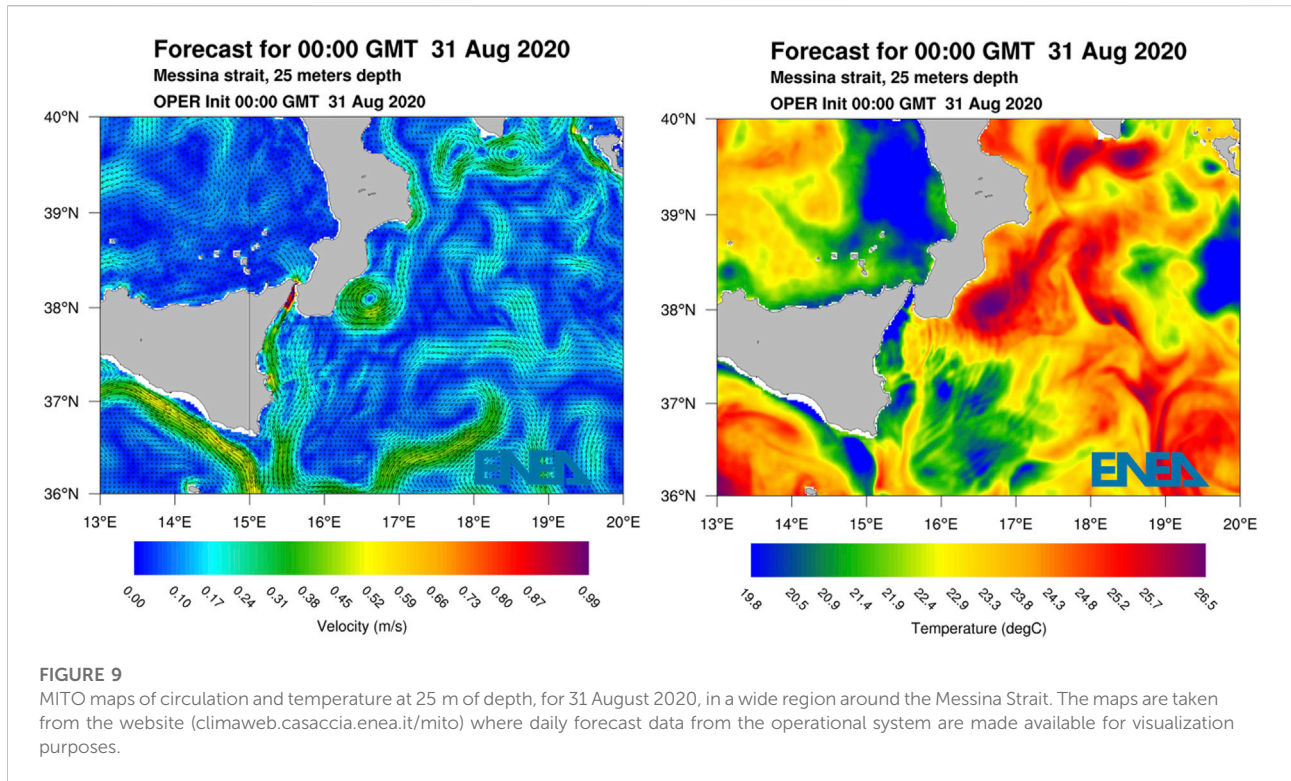
The model surface circulation is very similar to that derived from ADT data. The main feature in both fields is a westward coastal current, with a wide cyclonic circulation on the offshore side. This current is part of the wide cyclonic cell present in the northern portion of the western Mediterranean (Ligurian-Provençal basin). The model field has more details in the inner portion of the gulf, revealing a cyclone-anticyclone pair, with a smaller anticyclone near coast, to the west. Indications of the presence of these small-scale structures can be found in the turbidity map (K490; data from the CMEMS portal) of July 18th, shown in panel (c) of the figure. The image shows the presence of two coastal plumes in the inner part of the gulf. The westernmost plume bifurcates while heading towards south, with a branch that veers towards the coast, exactly in the region in which is the boundary of a small coastal anticyclone present in the model map. This small structure could not be resolved in the altimeter maps. On the other hand, the small eastern branch may be consistent with the presence of the anticyclonic pole of the dipole previously noted. The strongest plume, which corresponds to the outflow of the Rhone river, is also initially directed southward, but then gets trapped by the westward current; the main branch veers towards south-west, and a small branch towards south-east, bordering the wide cyclonic circulation present both in the ADT and model maps.

FIGURE 7
Average ADT maps in the Ionian region, for the years 2018 **(A)** 2019 **(B)** and 2020 **(C)**, with the corresponding geostrophic circulations superimposed. The anticyclonic cell still present in the northern Ionian in 2018 is rapidly destroyed.

FIGURE 8
Average July surface circulation in the area of the Gulf of Lion: **(A)** ADT (colors), with a geostrophic reconstruction of the circulation superimposed (AVISO, satellite data); **(B)** MITO currents at 10 m; **(C)** map of K490 (coefficient of light extinction at 490 nm) measured from satellite, for July 18.

Overall, this example indicates that the model is indeed capable of capturing mesoscale structures with sizes of few tens of kilometers.

Another area in which the description of small-scale dynamics is crucial is the Messina Strait, where the dynamics are deeply influenced by the tidal forcing. It has been shown in Palma et al. (2020) that MITO correctly describes the tidal dynamics in the area, and, despite the

non-optimal resolution, is capable of reproducing the strong currents observed inside the strait, which can exceed 2 m/s. Figure 9 shows maps of the circulation and temperature, at 25 m of depth, for 31 August 2020, in the area surrounding the strait, taken from the site in which results from the operational system are displayed, and constantly updated (https://climaweb.casaccia.enea.it/en/MITO/). The small red patch just south of the strait marks a strong tidally

FIGURE 9
MITO maps of circulation and temperature at 25 m of depth, for 31 August 2020, in a wide region around the Messina Strait. The maps are taken from the website (climaweb.casaccia.enea.it/mito) where daily forecast data from the operational system are made available for visualization purposes.

modulated current that then flows along most of Sicily's eastern coast (see Bohm et al., 1987, for experimental observations of the dynamics in the area). In the same region, the map of temperature shows the presence of a cold tongue that appears to originate in the southeastern corner of the Tyrrhenian Sea. Another interesting feature revealed by the temperature map is the presence of a wave-train that propagates towards south-east in the Ionian Sea.

Sea level

Comparison with absolute dynamic topography data

The sea surface elevation predicted by the model was compared with the AVISO altimetric data, which integrates data from all the available altimeters on board of different satellites, to yield ADT maps covering the Mediterranean Sea and part of the Atlantic and of the North Sea, at a uniform spatial resolution of 1/8° (about 14 km), both in latitude and longitude.

We have compared the weekly series of modelled elevation anomalies (with respect to the annual mean) to the corresponding series of mean ADT anomalies. Although daily data are in fact available, we have chosen to use weekly averages, because spectral analysis of the ADT time series shows no significant component with periods below 7–10 days.

A quantitative measure of the agreement between the observed and modelled elevation is provided by the map of the pointwise time correlation between the two time series, which is displayed in the top panel of Figure 10. In the lower panel of the same figure is the map of the 2020 ADT error obtained from AVISO data. The figure shows that the correlation is high (about 0.6 or more) in most of the basin, and highest in the eastern Mediterranean. There are small areas, particularly in the western basin, with low values of the correlation, located along the paths of the main currents systems (Algerian Current, Tyrrhenian Northern Current, Liguro-Provencal current, Atlantic stream in the Sicily Strait). This indicates that significant high frequency mesoscale variability associated with these currents is not fully captured by the altimeter observations. It should also be noted that some regions of low correlation correspond to regions with higher values of the ADT error, e.g., Algerian basin). We finally note that another possible reason for low correlation is that the model does not include the steric component, which can be locally important. Considering all these limitations, the agreement with the observations can be considered as satisfactory.

Table 4 shows regional averages (over the eight regions defined in Figure 2) of the RMSD and of the time correlation, which show consistency, since lower values of the RMSD and higher values of the correlation are found in the eastern basin. The RMSD values are just a little higher than the typical values for the Copernicus operational model, where the comparison between observed and simulated values was made along the satellite tracks.
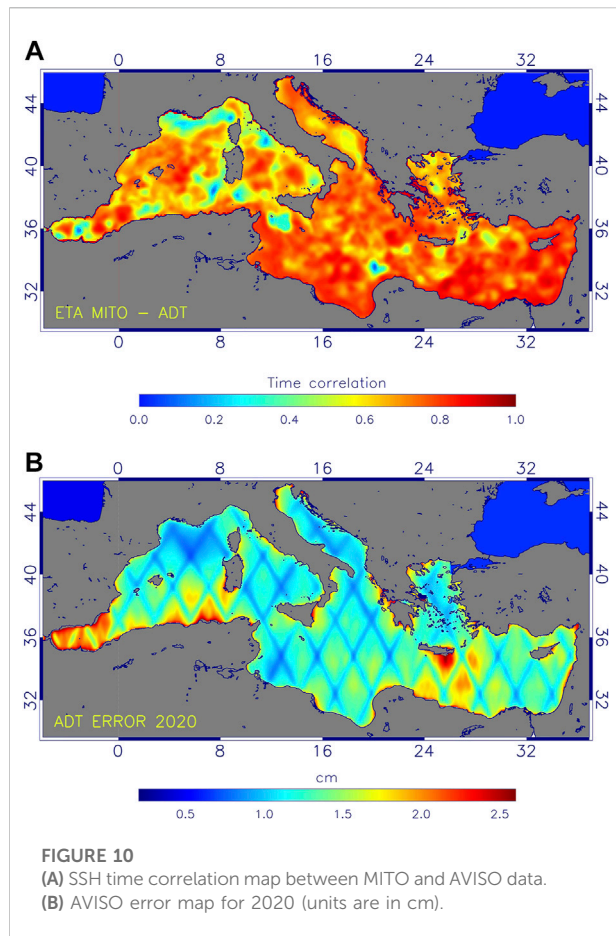
FIGURE 10
(A) SSH time correlation map between MITO and AVISO data.
(B) AVISO error map for 2020 (units are in cm).

TABLE 4 RMSD between the free surface of MITO and AVISO data (SSH anomaly).

Region	RMSD (cm)	Time correl
1	6.01	0.62
2	5.67	0.63
3	5.33	0.62
4	5.12	0.71
5	5.41	0.74
6	6.34	0.67
7	5.85	0.70
8	5.46	0.76

Coastal sea level

The predicted sea level heights were compared with the tide gauge measurements available for 2020 (55 stations, see left top panel of Figure 11). The 2020 observations are concentrated in the western Mediterranean and all along the Italian coasts.

Comparisons were made using the model grid point closest to the station, at the time closest to that measured.

The other panels of Figure 11 show histograms of the correlation coefficients between model and observed data, for the four seasons; in most of the cases the coefficients are higher than 0.85. This seems a very good result, considering that the model grid points can be quite far from the stations, and that the local bathymetry is not resolved with great detail.

By way of example, we show in the left lower panels of the figure the comparison between the time series of measured and observed elevation in four of the stations, for the month of January in SanBenedetto del Tronto and Sciacca, June in Porto Cristo, and July in Cagliari.

Tidal effects

The tidal behavior has been thoroughly investigated in Palma et al. (2020), where it has been shown that the model reproduces both the barotropic and the baroclinic tide very well. It was also shown in that work that tides significantly modulate the transport, not only through the Strait of Gibraltar and the Strait of Sicily, but also through the Corsica Channel and the Strait of Otranto. The tidal effects also modify some characteristics of the circulation inside the basin; in some cases, topographic waves are excited and get trapped by the bathymetry, producing diurnal rotations of the currents. Examples of this phenomenon have been found in the Sicily Channel (on the Adventure Bank and on the Malta Plateau), in the Corsica Channel and in the Strait of Otranto. Furthermore, in different areas of the basin (Channel of Sicily, Channel of Corsica, Strait of Messina, Northern Adriatic Sea), spectral analysis of the average kinetic energy reveals the presence of spectral peaks corresponding to periods of approximately 8 and 6 h, which can be interpreted as harmonics (overtides and compounds) of the diurnal and semi-diurnal tide components, generated through non-linear interactions.

We have found similar results analyzing the 2020 forecasts. For example, the mean kinetic energy power spectrum (not shown) for the region over the Adventure Bank shows dominant diurnal components, which are accompanied by significant semidiurnal components, and also by quite strong peaks corresponding to nonlinear harmonics (periods of 8 and 6 h).

Conclusion

We have described the main features of MITO, a new operational system for the forecasting of the Mediterranean circulation that is running since 2018, and performed a detailed evaluation of its performances, by comparing the forecasts of the year 2020 with a variety of experimental data.
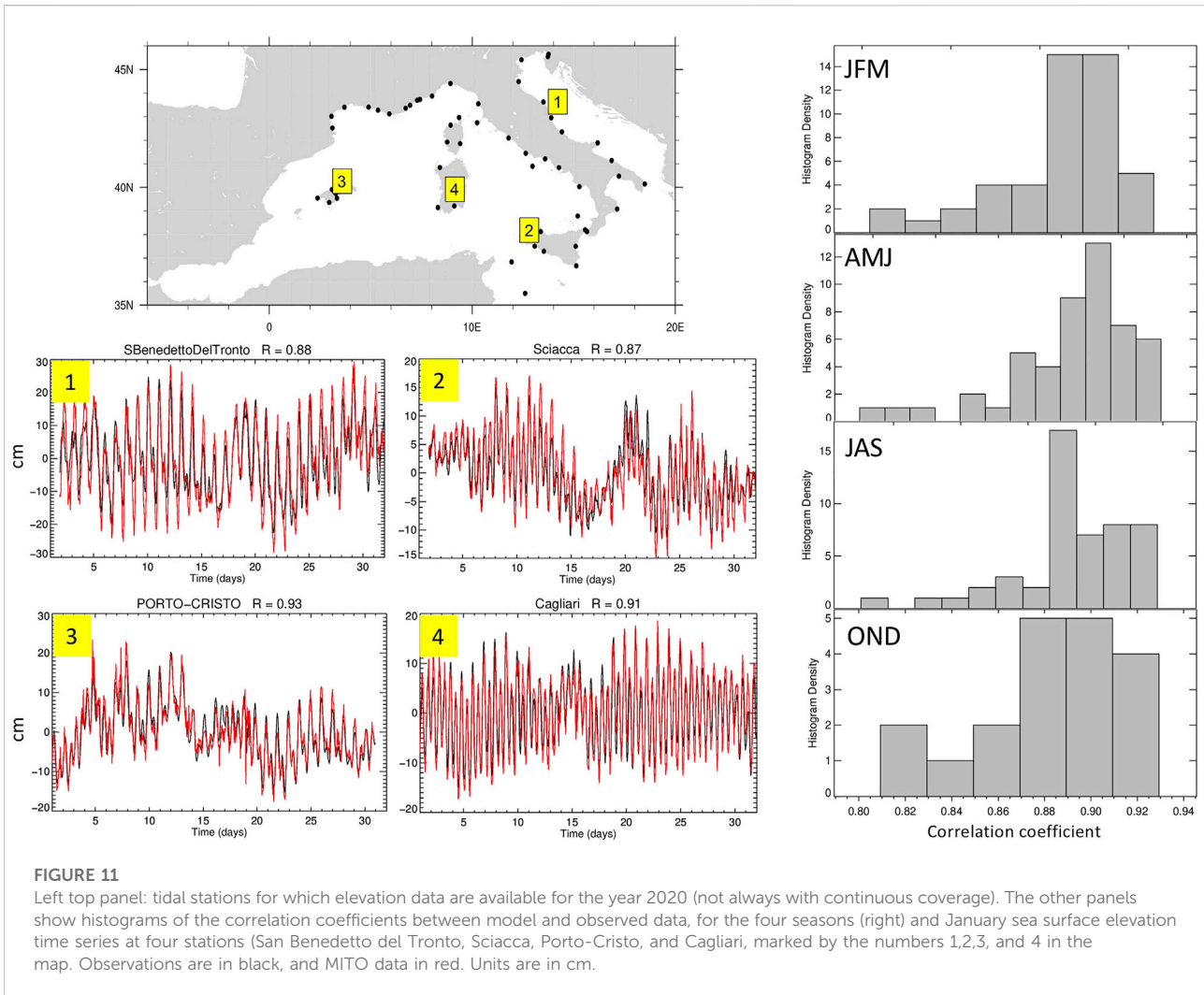
FIGURE 11
Left top panel: tidal stations for which elevation data are available for the year 2020 (not always with continuous coverage). The other panels show histograms of the correlation coefficients between model and observed data, for the four seasons (right) and January sea surface elevation time series at four stations (San Benedetto del Tronto, Sciacca, Porto-Cristo, and Cagliari, marked by the numbers 1,2,3, and 4 in the map. Observations are in black, and MITO data in red. Units are in cm.

The model-data comparison revealed that the hydrological structure and the circulation are generally in good agreement with the observations. The model was also found to correctly reproduce robust mesoscale structures, and the tide-induced sea level variability in coastal areas. This indicates that the MITO system could be successfully used to nest higher resolution coastal models.

There are aspects that could be improved, and will be the object of future development. The first naturally concerns the inclusion of data assimilation, which could improve the quality of the initial conditions. We have found that the surface temperature shows a larger bias (albeit generally well below 1°C) during the summer phase. This may be due to various problems, including for example the quality of the atmospheric forcing, especially for what concerns the short-wave radiation, which is the component of the total heat flux that modulates the diurnal variability of the SST. Other errors could contribute to the cold bias, such as atmospheric forecast errors due to a bad cloud cover representation or to numerical schemes. Note also

that the diurnal SST cycle reproduced by the model is in qualitative agreement with the observation, but with a smaller range of variation. Another issue that could be interesting to consider is the fact that the extinction coefficient of short-wave radiation, which is here taken as constant, as it is usually done, may instead have seasonal and regional variability. Satellite products could be of help in addressing this issue. Salinity in the surface layer has also been found to have a bias with respect to experimental data in some regions, indicating that the components of the E-P-R budget should be further examined to improve the agreement with the observations. The inclusion of additional tidal components could also be envisaged, to have a more complete representation of the tidal forcing.

Nevertheless, we believe that the MITO system, thanks to its high resolution and to the capability of describing the linear and nonlinear dynamics induced by tidal forcing, may represent a useful tool in support of a wide spectrum of applications focusing on coastal areas, including energy extraction.

We finally note that the archive of short-term forecasts produced through the years, providing a long-term, high-resolution description of the evolution of the Mediterranean dynamics, will allow in the future for the investigation of the basin variability on time scales of climatic interest. Such archive could also be used as a training set for machine learning applications, for the exploration of alternative forecasting approaches.

Data availability statement

The raw data supporting the conclusions of this article will be made available by the authors, without undue reservation.

Author contributions

GS and AC: implemented the model. EL: performed the run, GS, RI, AC, EN, GP, MVS, and MP: designed the analysis, RI, AC, MP, and EN: performed the analysis. All the authors contributed to writing the paper.

Acknowledgments

Conflict of interest

The authors declare that the research was conducted in the absence of any commercial or financial relationships that could be construed as a potential conflict of interest.

Publisher's note

All claims expressed in this article are solely those of the authors and do not necessarily represent those of their affiliated organizations, or those of the publisher, the editors and the reviewers. Any product that may be evaluated in this article, or claim that may be made by its manufacturer, is not guaranteed or endorsed by the publisher.

References

Barbarelli, S., Florio, G., Amelio, M., and Scornaienchi, N. M. (2018). Preliminary performance assessment of a novel on-shore system recovering energy from tidal currents. *Appl. Energy* 224, 717–730. doi:10.1016/j.apenergy.2018.05.029

Bohm, E., Magazzu, G., Wald, L., and Zoccolotti, M. L. (1987). Coastal currents on the Sicilian shelf south of Messina. *Oceanol. Acta* 10 (2), 137–142.

Borzelli, G., Gacic, M., and Civitarese, G. (2009). Eastern mediterranean transient and reversal of the Ionian Sea circulation. *Geophys. Res. Lett.* 36 (15). doi:10.1029/2009GL039261

Buongiorno Nardelli, B., Tronconi, C., Pisano, A., and Santoleri, R. (2013). High and ultra-high resolution processing of satellite Sea surface temperature data over southern European seas in the framework of MyOcean project. *Remote Sens. Environ.* 129, 1–16. doi:10.1016/j.rse.2012.10.012

Clementi, E., Aydogdu, A., Goglio, A. C., Pistoia, J., Escudier, R., Drudi, M., et al. (2021). *Mediterranean Sea analysis and forecast (CMEMS MED-currents, EAS6 system) (version 1) [data set]*. Copernicus Monitoring Environment Marine Service (CMEMS). doi:10.25423/CMCC/MEDSEA_ANALYSISFORECAST_PHY_006_013_EAS6

Coiro, D. A. P., Troise, G., Ciuffardi, T., and Sannino, G. (2013). "Tidal current energy resource assessment: the strait of Messina test case," in *International conferencs on clean electrical power (ICCEP)* (Alghero,Italy: IEEE), 213–220.

Davidson, F., Alvera-Azcárate, A., Barth, A., Brassington, G. B., Chassignet, E. P., Clementi, E., et al. (2019). Synergies in operational oceanography: The intrinsic need for sustained ocean observations. *Front. Mar. Sci.* 6, 450. doi:10.3389/fmars.2019.00450

de Ruggiero, P., Napolitano, E., Iacono, R., and Pierini, S. (2016). A high-resolution modelling study of the circulation along the Campania coastal system, with a special focus on the Gulf of Naples. *Cont. Shelf Res.* 122, 85–101. doi:10.1016/j.csr.2016.03.026

Doney, S. C., Nijar, R., and Stewart, S. (1995). Photochemistry, mixing and the diurnal cycles in the upper ocean. *J. Mar. Res* 53, 341–369.

Ezer, T., and Mellor, G. L. (1994). Diagnostic and prognostic calculations of the North Atlantic circulation and sea level using a sigma coordinate ocean model. *J. Geophys. Res.* 99 (7), 14159–14171. doi:10.1029/94JC00859

Fernandez, V., Lara-Lopez, A., Eparkhina, D., Cocquempot, L., Lochet, C., and Lips, I. (Editors) (2021). "Advances in operational oceanography: Expanding Europe's ocean observing and forecasting capacity," in Proceedings of the 9th

EuroGOOS International Conference, Brussels, Belgium, May 3–5, 2021 (EuroGOOS), 574 pp. Available at: https://archimer.ifremer.fr/doc/00720/83160/ [Online].

Kallos, G., Papadopoulos, A., Katsafados, P., and Nickovic, S. (2006). Transatlantic saharan dust transport: Model simulation and results. *J. Geophys. Res.* 111, D09204. doi:10.1029/2005JD006207

Kallos, G., Nickovic, S., Papadopoulos, A., Jovic, D., Kakaliagou, O., Misirlis, N., et al. (1997). "The regional weather forecasting system SKIRON: An overview," in *Proceedings of the symposium on regional weather prediction on parallel computer environments* Editor B. George, V. Kallos, and K. Kotroni (Athens, Greece: Lagouvardos), 109–122.

Marshall, J., Hill, C., Perelman, L., and Adcroft, A. (1997a). Hydrostatic, quasi-hydrostatic, and nonhydrostatic ocean modeling. *J. Geophys. Res.* 102, 5733–5752. doi:10.1029/96jc02776

Marshall, J., Adcroft, A., Hill, C., Perelman, L., and Heisey, C. (1997b). A finite-volume, incompressible Navier Stokes model for studies of the ocean on parallel computers. *J. Geophys. Res.* 102, 5753–5766. doi:10.1029/96jc02775

Marullo, S., Minnet, P. J., Santoleri, R., and Tonani, M. (2016). The diurnal cycle of sea-surface temperature and estimation of the heat budget of the Mediterranean Sea. *J. Geophys. Res. Oceans* 121 (11), 8351–8367. doi:10.1002/2016jc012192

Menna, M., Reys Suarez, N. C., Civitarese, G., Gačić, M., Rubino, A., and Poulain, P. M. (2019). Decadal variations of circulation in the Central Mediterranean and its interactions with mesoscale gyres. *Deep Sea Res. Part II Top. Stud. Oceanogr.* 164, 14–24. doi:10.1016/j.dsr2.2019.02.004

Napolitano, E., Iacono, R., and Marullo, S. (2014). "The 2009 surface and intermediate circulation of the Tyrrhenian Sea as assessed by an operational model," in *The Mediterranean Sea: Temporal variability and spatial pat- terns, geophysical monograph*. Editors G. L. E. Borzelli, M. Gacic, P. Lionello, and P. Malanotte-Rizzoli. 1st ed. (Washington DC: American Geophysical Union, published by Wiley), 59–74.

Napolitano, E., Iacono, R., Sorgente, R., Fazioli, L., Olita, A., Cucco, A., et al. (2016). The regional forecasting systems of the Italian seas. *J. Operational Oceanogr.* 9, s66–s76. doi:10.1080/1755876X.2015.1117767

Naranjo, C., Garcia-Lafuente, J., Sannino, G., and Sanchez-Garrido, J. C. (2014). How much do tides affect the circulation of the Mediterranean Sea? From local processes in the strait of Gibraltar to basin-scale effects. *Prog. Oceanogr.* 127, 108–116. doi:10.1016/j.pocean.2014.06.005

Nikolaidis, G., Karaolia, A., Matsikaris, A., Nikolaidis, A., Nicolaides, M., and Georgiou, G. C. (2019). Blue energy potential analysis in the mediterranean. *Front. Energy Res.* 7, 62. doi:10.3389/fenrg.2019.00062

Notarstefano, G., Menna, M., and Legas, F. (2019). Reversal of the northern ionian circulation in 2017. *J. Ope. Oce* 1, 108–111. Copernicus Marine Service Ocean State Report, Issue 3. doi:10.1080/1755876X.2019.1633075

Oddo, P., Adani, M., Pinardi, N., FratianniTonani, C, M., and Pettenuzzo, D. (2009). A nested Atlantic-Mediterranean Sea general circulation model for operational forecasting. *Ocean. Sci.* 5, 461–473. doi:10.5194/os-5-461-2009

Palma, M., Iacono, R., Sannino, G., Bargagli, A., ACarillo, A., Fekete, M., et al. (2020). Short-term, linear, and non-linear local effects of the tides on the surface dynamics in a new, high-resolution model of the Mediterranean Sea circulation. *Ocean. Dyn.* 70, 935–963. doi:10.1007/s10236-020-01364-6

Papadopoulos, A., and Katsafados, P. (2009). Verification of operational weather forecasts from the POSEIDON system across the Eastern Mediterranean. *Nat. Hazards Earth Syst. Sci.* 9, 1299–1306. doi:10.5194/nhess-9-1299-2009

Pisacane, G., Sannino, G., Carillo, A., Struglia, M. V., and Bastianoni, S. (2018). Marine energy exploitation in the mediterranean region: Steps forward and challenges. *Front. Energy Res.* 6, 109. doi:10.3389/fenrg.2018.00109

Sannino, G., Carillo, A., Pisacane, G., and Naranjo, C. (2015). On the relevance of tidal forcing in modelling the Mediterranean thermohaline circula- tion. *Prog. Oceanogr.* 134, 304–329. doi:10.1016/j.pocean.2015.03.002

Schiller, A., and Brassington, G. B. (Editors) (2011). *Operational oceanography in the 21st century* (Dordrecht, Netherlands: Springer). doi:10.1007/978-94-007-0332-2

Stathopoulos, C., Kaperoni, A., Galanis, G., and Kallos, G. (2013). Wind power prediction based on numerical and statistical models. *J. Wind Eng. Industrial Aerodynamics* 112, 25–38. doi:10.1016/j.jweia.2012.09.004

Zhang, T. L., Xiao, R., Cao, Q., Zhang, Y., Qu, Q., Wang, Z., et al. (2022). Interactive effects of ocean acidification, ocean warming, and diurnal temperature cycling on antioxidant responses and energy budgets in two sea urchins Strongylocentrotus intermedius and Tripneustes gratilla from different latitudes. *Sci. Total Environ.* 824. doi:10.1016/j.scitotenv.2022.153780